BMC Endocrine Disorders

CASE REPORT Open Access

Tumor-induced osteomalacia characterized by "painful knee joint with difficulty in moving": a case report

Lan Jiang[1†], Qing-Qing Tan[1,2,3,4†], Chen-Lin Gao[1,2,3,4], Ling Xu[1], Jian-Hua Zhu[1], Pi-Jun Yan[1], Ying Miao[1], Qin Wan[1*] and Yong Xu[1,2,3,4*]

Abstract

Background: Tumor-related osteomalacia (TIO) is a rare paraneoplastic syndrome characterized by severe hypophosphatemia and osteomalacia. The diagnosis of TIO can be very difficult because of its nonspecific nature of clinical manifestations. Here we reported a case of young TIO patient with "painful knee joint with difficulty in moving" to improve the clinical diagnosis and treatment levels.

Case presentation: The patient's clinical features were consistent with TIO. A tumor was successfully located in left tibial by ^{68}Ga-DOTATATE PET/CT, and then was surgically resected. Upon pathologic assessment, the tumor was diagnosed as phosphaturia stromal tumor (PMT) with positive Vim staining. After the surgery, serum phosphate level rapidly recovered and symptoms significantly improved.

Conclusion: TIO should be considered in patients with chronically hypophosphorus osteomalacia in the setting of no family history. Early removal of the responsible tumors is clinically essential for the treatment, and imaging examination is of great significance for tumor localization.

Keywords: Tumor-induced osteomalacia, Fibroblast growth factor-23, Hypophosphatemia, ^{68}Ga DOTATATE PET/CT, Case report

Background

TIO is a rare paraneoplastic syndrome caused by tumors that ectopically overproduce fibroblast growth factor-23 (FGF-23), leading to decreased renal tubular reabsorption of phosphate. It is characterized by severe hypophosphatemia and osteomalacia [1]. Symptoms of TIO vary but mainly are gradually progressive bone pain and muscle weakness, pathological fracture and height shorten in severe cases [2]. It was first reported by Mccance in 1947, and less than 500 cases have been reported worldwide till now [3]. The diagnosis of TIO can be very difficult because of its insidious onset and nonspecific nature of clinical manifestations. The longer the course of the disease, the higher the disability rate [4]. Therefore, we described a TIO patient with "painful knee joint with difficulty in moving" as the typical manifestation and reviewed relevant literatures, in order to improve the recognition of this rare disease.

Case presentation

Case history

The 22-year-old female patient was admitted to the hospital on August 25, 2021 with the chief complaint

†Lan Jiang and Qing-Qing Tan are co-first author.

†Lan Jiang and Qing-Qing Tan contributed equally to this work.

*Correspondence: wanqin3@163.com; xywyll@swmu.edu.cn

[1] Department of Endocrinology and Metabolism, The Affiliated Hospital of Southwest Medical University, Luzhou 646000, Sichuan, China
Full list of author information is available at the end of the article

© The Author(s) 2022. **Open Access** This article is licensed under a Creative Commons Attribution 4.0 International License, which permits use, sharing, adaptation, distribution and reproduction in any medium or format, as long as you give appropriate credit to the original author(s) and the source, provide a link to the Creative Commons licence, and indicate if changes were made. The images or other third party material in this article are included in the article's Creative Commons licence, unless indicated otherwise in a credit line to the material. If material is not included in the article's Creative Commons licence and your intended use is not permitted by statutory regulation or exceeds the permitted use, you will need to obtain permission directly from the copyright holder. To view a copy of this licence, visit http://creativecommons.org/licenses/by/4.0/. The Creative Commons Public Domain Dedication waiver (http://creativecommons.org/publicdomain/zero/1.0/) applies to the data made available in this article, unless otherwise stated in a credit line to the data.

of "double knee joints pain for 10+ years, aggravation for 2+ months, accompanied by groin pain for 2+ weeks". 10+ years ago, she had recurrent pain in both knees without obvious inducement, occasionally with knee valgus and knee dislocation. 2+ years ago, she developed low back pain which was relieved after rest, but the spine moved freely. 1+ years ago, she experienced severe pain in her low back and loss of mobility. She needed help to get up and down stairs, usually could only walk slowly. 2+ months ago, the pain became progressively worse and she developed pain in the groin area and the right 12th rib after a tumble. MRI showed bone marrow edema in the right intertrochanteric, femoral neck, lower left femur, and tibial intercondylar crest. 2+ weeks ago, she had occasional wandering pain of joints all over the body, accompanied by difficulty in walking and increased pain after weight bearing. Biochemical tests revealed hypophosphatemia (0.47 mmol/L), high serum alkaline phosphatase (257 IU/L), low 25-OH Vit D (41.1 nmol/L), and dual-energy X-ray absorptiometry (DXA) demonstrated reduced bone density. Then she was admitted into the Department of Endocrinology of our hospital for further treatment. She had lost 3 cm in height over 10 years. Her medical history included polycystic ovary syndrome (PCOS) for nearly 3 years, with irregular menstruation. Deny bad eating habits, long-term absence from sunlight, chronic diarrhea and the history of taking adefovir dipivoxil or other drugs. No history of recurrent skin hemorrhages or tooth loss or fracture. No family history of skeletal, metabolic or hormonal disorders.

Physical examination

She is 142 cm tall and weighs 46 kg, with no obvious positive signs in heart, lung and abdominal examination. Lower limbs are unequal in length and circumference (Relative length of lower limbs: R 77.5 cm, L 76 cm; absolute length of lower limbs: R 68 cm, L 67 cm. Thigh circumference: R 47.5 cm, L 45.5 cm; calf circumference: R 37.5 cm, L 33.5 cm) (Table 1). Physical examination reveales scoliosis deformity without tenderness and percussion pain in spinous process, hip flexion, extension, internal and external rotation (+), adduction, abduction (−), Moberg sign (+), Lasegue sign (−), both knee joints pain, limited movement, left knee joint evagination deformity, "X" shaped leg. No swelling, tenderness, dislocation of joints, no atrophy of muscles, no paralysis of limbs, no enhancement or weakening of muscle tension.

Table 1 Physical examination of the patient with tumor-induced osteomalacia (TIO)

Items	Relative length of lower limbs (cm)	Absolute length of lower limbs (cm)	Thigh circumference (cm)	Calf circumference (cm)
R	77.5	68	47.5	37.5
L	76	67	45.5	33.5

Preoperative laboratory examination (august 25, 2021)

(1) Alkaline phosphatase: 270.4 U/L (n: 35-100 U/L); (2) Phosphorus: 0.52 mmol/L (n: 0.85–1.51 mmol/L); (3) Calcium: 2.29 mmol/L (n: 2.11–2.52 mmol/L); (4) Magnesium: 0.91 mmol/L (n: 0.75–1.02 mmol/L); (5) Creatinine: 42.9umol/L (n: 41-73umol/L); (6) Calcitonin: 15.3 pg/ml (n: 0.0–18.0 pg/ml); (7) Parathyroid hormone: 61.23 pg/ml (n: 8.70–79.60 pg/ml); (8) 25-OH Vit D: 16.00 ng/ml (deficiency: < 20 ng/ml); (9) Total procollagen I N terminal peptide: 90.84 ng/ml (n: premenopausal 8.53–64.32 ng/ml; Postmenopausal 21.32–112.80 ng/ml); (10) β-Crosslaps: 623.40 pg/ml (n: premenopausal 68.00–680.00 pg/ml; postmenopausal 131.00–900.00 pg/ml); (11) N-MID osteocalcin: 15.30 ng/ml (n: premenopausal 4.11–21.87 ng/ml; postmenopausal 8.87–29.05 ng/ml) (Table 2).

Preoperative imaging examination

CT (August 30, 2021)

Old fractures of multiple ribs on both sides. Left ilium and left sacrum bone islands (Fig. 1).

Table 2 Preoperative laboratory examination findings of the patient

Items	Result	Reference range
Alkaline phosphatase (U/L)	270.4	35–100
Phosphorus (mmol/L)	0.52	0.85–1.51
Calcium (mmol/L)	2.29	2.11–2.52
Magnesium (mmol/L)	0.91	0.75–1.02
Creatinine (umol/L)	42.9	41–73
Calcitonin (pg/ml)	15.3	0.0–18.0
Parathyroid hormone (pg/ml)	61.23	8.70–79.60
25-OH Vit D (ng/ml)	16.00	deficiency: < 20
Total PINP (ng/ml)	90.84	8.53–64.32
β-Crosslaps (pg/ml)	623.40	68.00–680.00;
N-MID osteocalcin (ng/ml)	15.30	4.11–21.87 ng/ml;

PINP procollagen I N terminal peptide

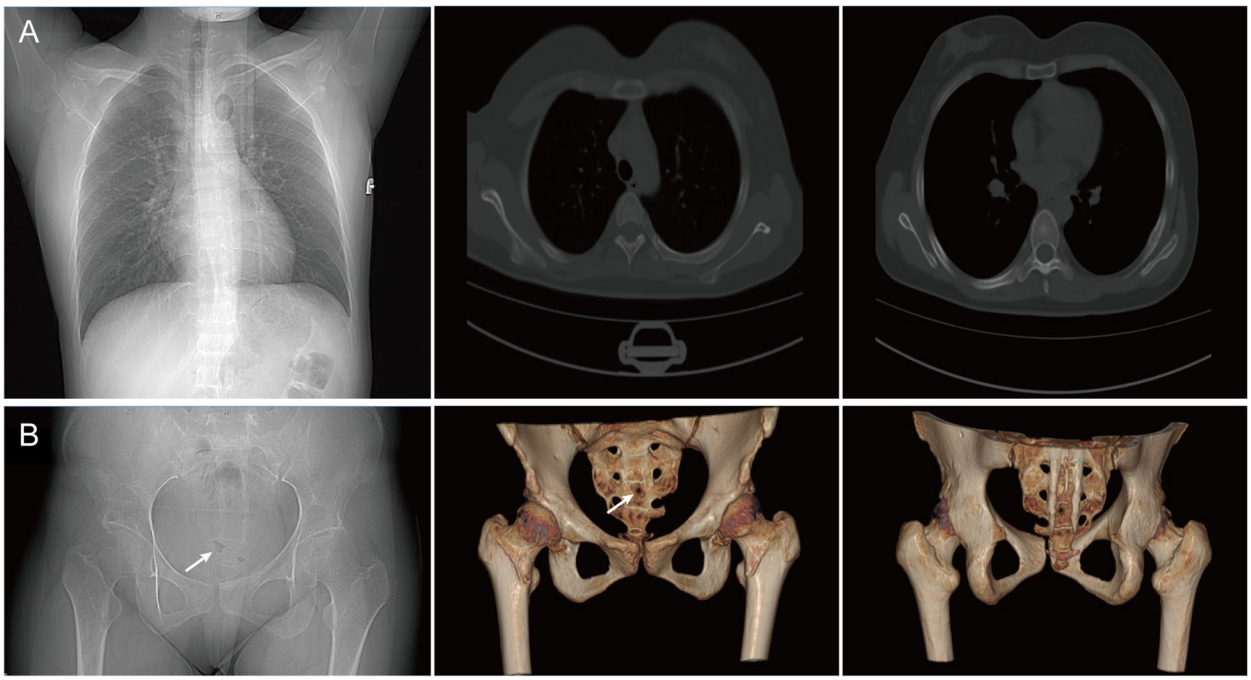

Fig. 1 CT imaging of this patient. **A** Chest CT shows bone structure disorder in multiple ribs on both sides. (**B**) Hip joint CT shows nodular high density in the left ilium and sacrum, the bone structure of the remaining two hip joints is intact

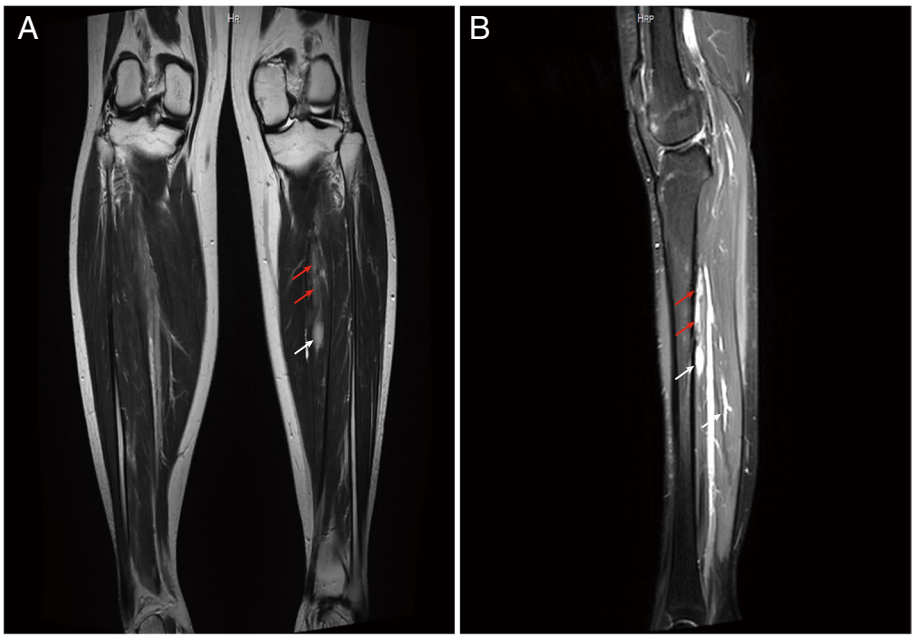

Fig. 2 MRI imaging of tumor-induced osteomalacia. MRI shows an elliptic slightly high signal near the cortical bone of the posterior edge of the left middle tibia (1.6*0.7 cm, indicated by the white arrow), and a small nodular, vertical strip abnormal signal outside the bone (1.5 cm, indicated by the red arrows). **A** Coronal MRI, **B** sagittal MRI

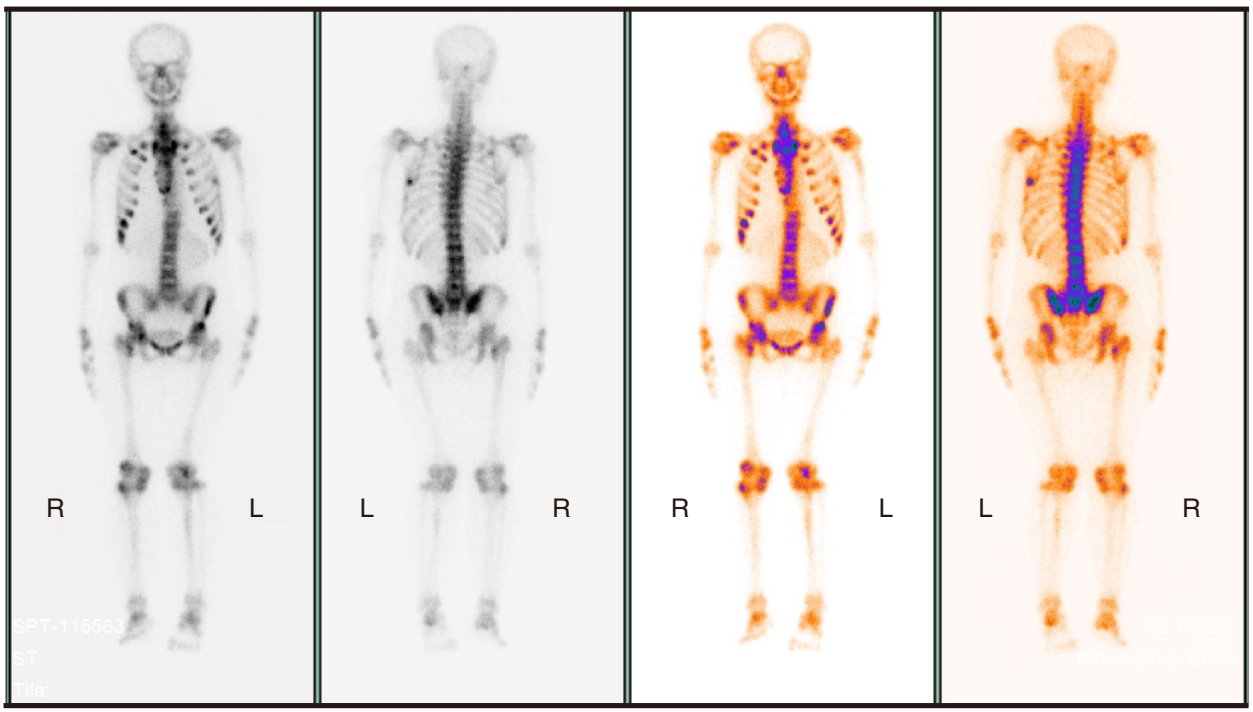

Fig. 3 ^{99m}Tc-MDP whole body bone scan. ^{99m}Tc-MDP whole body bone scan shows osteomalacia, with pseudo fractures of multiple ribs and right femoral neck

MRI (August 29, 2021)

An elliptic slightly high signal near the cortical bone of the posterior edge of the left middle tibia (1.6*0.7 cm), and a small nodular, vertical strip abnormal signal outside the bone (1.5 cm) (Fig. 2).

DXA (August 12, 2021)

L1-L2 −1.5; L1-L3 −1.5; L1-4 −1.7; L2-L3 −1.7; L2-L4 −1.8; L3-L4 −1.8; Neck −2.9; Wards triangle −2.7; Great trochanter −2.4; All −2.3.

^{99m}Tc-MDP bone scan (August 27, 2021)

Osteomalacia, with pseudo fractures of the anterior segment of the right 2nd rib, the axillary segment of the left 7th and 8th ribs, right side of the sacrum, left acetabulum, and right femoral neck (Fig. 3).

^{68}Ga-DOTATATE PET/CT (August 27, 2021)

Abnormal density of left middle and upper tibia with increased somatostatin receptors (SSTR) expression. Pseudo fracture of multiple ribs (the posterior segment of the left 5th rib, the axillary segment of the left 7th to 8th rib, the anterior segment of the right 2nd rib) and right femoral neck with increased SSTR expression. TIO was considered in the above lesions (Fig. 4).

Diagnosis and treatment

Combined with the above clinical history, physical examination, laboratory evaluation, the patient was initially confirmed to have TIO. The responsible tumor was located in the left proximal tibia. The patient then underwent resection and biopsy of the left tibial tumor on September 6, 2021. During the operation, there was a bony protrusion and bone destruction in the left proximal lateral tibia, and white soft tissue beside the bone. The damaged bone tissue and soft tissue beside the bone were taken and sent for pathological examination. Then we used Kirschner wire to drill holes in the lesion area, and used electric knife to kill the lesion tissue at high temperature. Postoperative histopathological examination demonstrated a spindle cell tumor with prominent vascularity, smoky matrix, "grungy" calcification and a small amount of multinucleated, osteoclast-like giant cells (Fig. 5). Immunohistochemical staining was also performed, and the results are as follows: Vim (+), SATB2 (partly+), CD34 (−), S100 (−), Desmin (−), SMA (−), P53 (−), Ki-67 (positive rate, 1%), STAT6 (−), AE1/AE3 (PCK) (−), compatible with a PMT (Fig. 6). By postoperative day 5, the serum phosphorus normalized (0.94 mmol/L) and symptoms improved (Fig. 7 and Table 3). And now the patient's systemic bone pain has improved significantly.

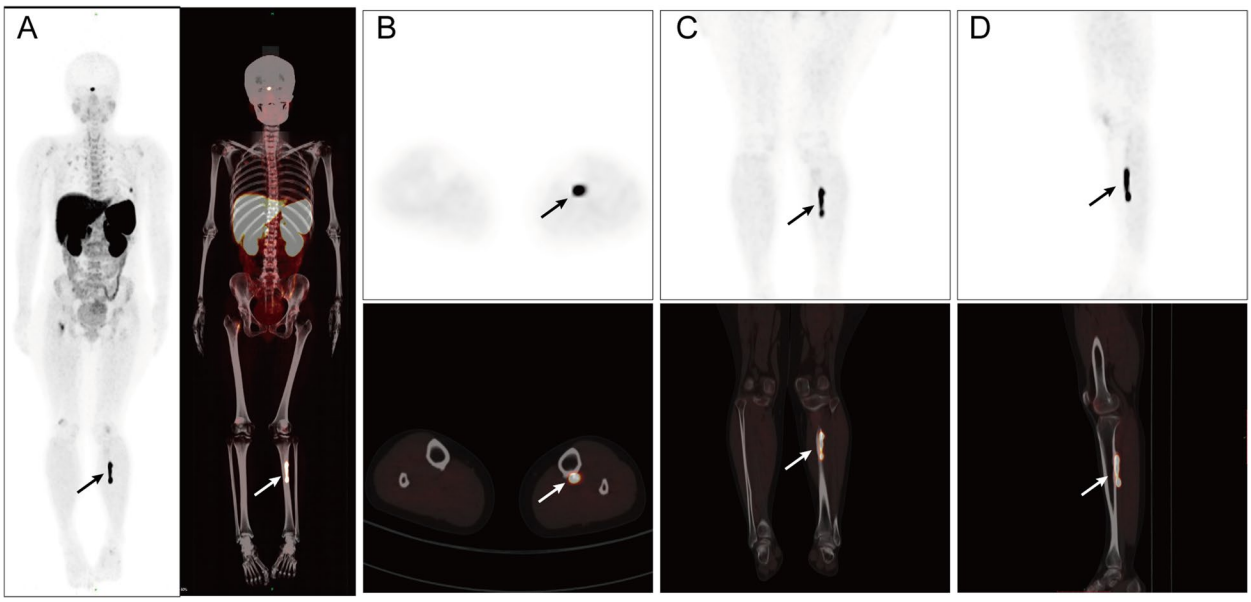

Fig. 4 ^{68}Ga-DOTATATE PET/CT imaging of tumor-induced osteomalacia. ^{68}Ga-DOTATATE PET/CT shows abnormal density of left middle and upper tibia with increased SSTR expression. Pseudo fracture of multiple ribs and right femoral neck with increased SSTR expression

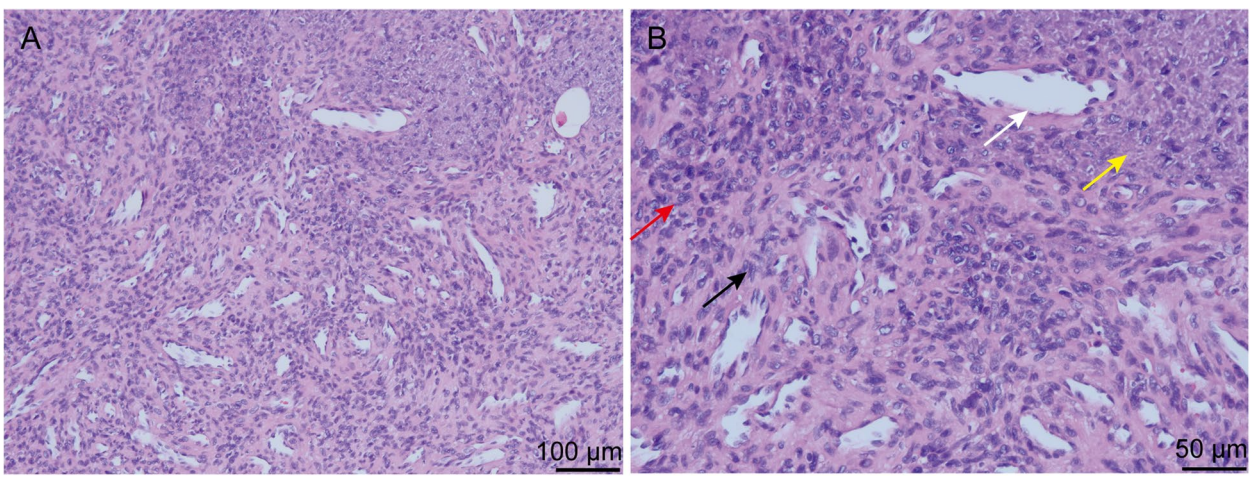

Fig. 5 The histological features of phosphaturic mesenchymal tumor (PMT). Low-magnification (**A,** 100×) and high magnification (**B,** 200×) images of a PMT. Highly vascular proliferation (indicated by the white arrow) and spindle-shaped cells (indicated by the black arrow) form most of the background cells and are embedded in a distinctive smudgy matrix. The osteoclast-like multinucleated giant cells (indicated by the red arrow) and "grungy" calcification are scattered in the tumor (indicated by the yellow arrow)

Discussion and conclusions

TIO is an acquired metabolic bone disease caused by tumor, and is one of causes of osteomalacia hypophosphorus in adults. Laboratory tests in TIO show refractory hypophosphatemia, elevated alkaline phosphatase, reduced tubular reabsorption of phosphate, low or normal $1,25(OH)_2D$, serum calcium and parathyroid hormone [2, 5]. Most studies believed that TIO is caused by phosphorus-regulating factors secreted by responsible tumors [6]. Among them, FGF23 is the only protein that has been shown to have clinical significance, which results in hypophosphatemia and renal phosphate wasting, reduced $1,25(OH)_2D$ synthesis, and osteomalacia [7]. Klotho, as a coreceptor for FGF23, mediates various

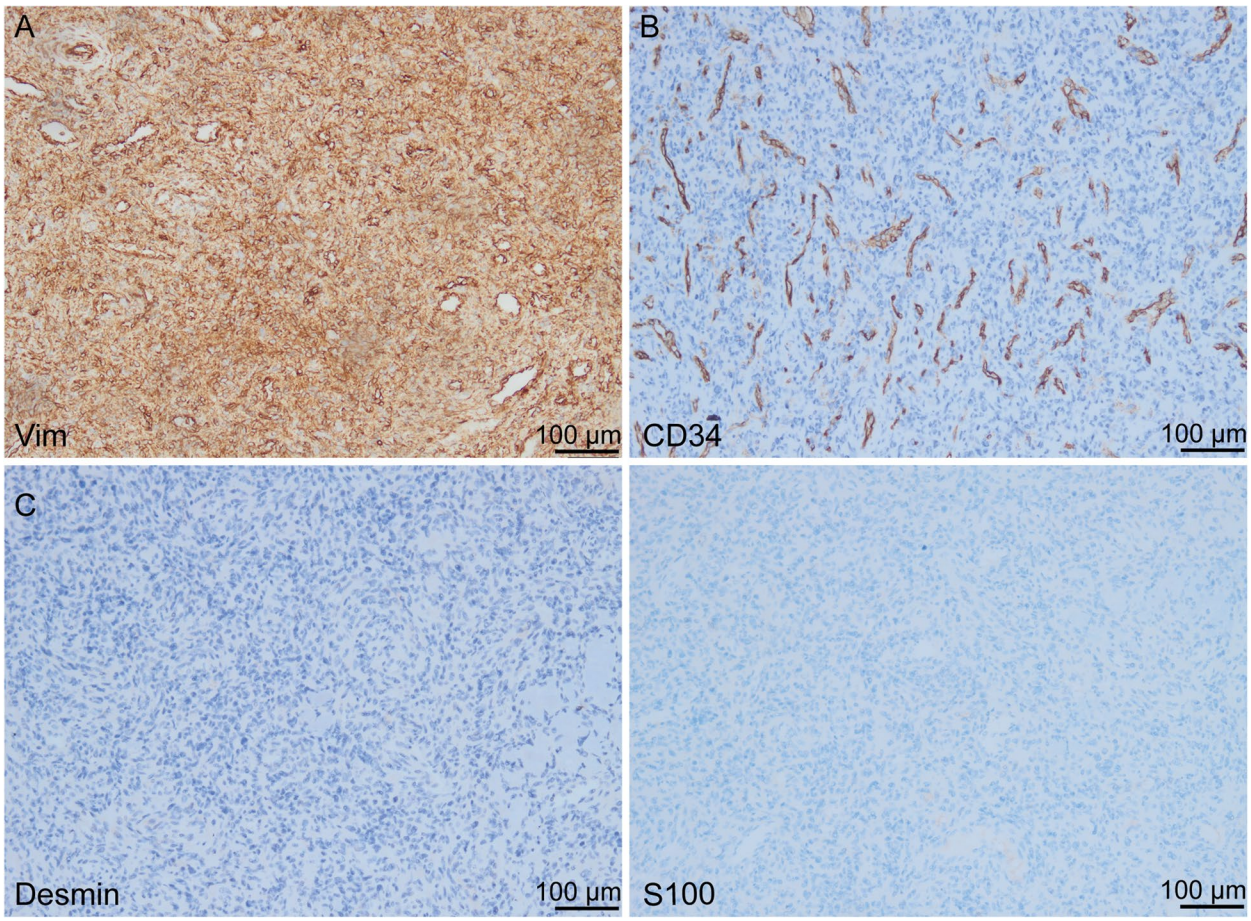

Fig. 6 Immunohistochemisty for Vim, CD34, Desmin, and S100 of the tumor (100×). **A** Vim, as a mesenchymal cell marker, is positive in most tumor cells, indicating the tumor originated from mesenchymal tissues (brown). **B** The tumor contains a large number of small capillaries, most of which are positive for CD34 staining (brown) whereas tumor cells are negative. **C** Desmin is characteristically found in muscle cells and associated neoplasms, is negative in PMT. **D** S100 is the specific protein of neural crest-derived tumors, is negative in PMT

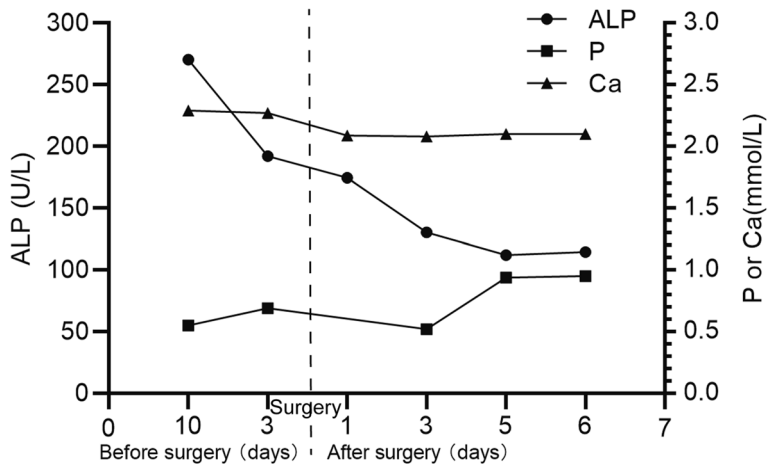

Fig. 7 Changes of the serum alkaline phosphatase (ALP), serum phosphate (P), and serum calcium (Ca) before and after surgery. Hypophosphatemia was rapidly improved, and phosphate levels returned to normal within 5 days. However, the elevated serum ALP and the mild hypocalcemia was not improved in the short term

Table 3 Changes of the serum alkaline phosphatase (ALP), serum phosphate (P), and serum calcium (Ca) before and after surgery

Time (days)	Before surgery		After surgery			
	10d	3d	1d	3d	5d	6d
ALP (U/L) (n: 35–100)	270.4	192.1	174.5	130.3	112.1	114.7
P (mmol/L) (n: 0.85–1.51)	0.55	0.69	NA	0.52	0.94	0.95
Ca (mmol/L) (n: 2.11–2.52)	2.29	2.27	2.09	2.08	2.10	2.10

Hypophosphatemia was rapidly improved, and phosphate levels returned to normal within 5 days. However, the elevated serum ALP and the mild hypocalcemia was not improved in the short term. *NA* Not available

physiological processes to maintain phosphate and calcium homeostasis. There are different isoforms of Klotho protein: membrane-bound Klotho and soluble Klotho [8]. The ectopic expression of membrane-bound Klotho in PMTs enables a positive feedback loop in FGF23 production via the activation of FGF receptor 1c and exacerbates disease manifestations in TIO [9]. Soluble αKlotho fragment that is produced by ectodomain shedding can circulate in the blood, urine and cerebrospinal fluid [10]. However, the function and mechanism of circulating soluble Klotho in FGF23-producing tumors that cause TIO is yet to be clarified. TIO-associated tumors are usually reported to be PMT that is mostly benign tumors derived from mesenchymal tissue [11]. Histologically, PMT are composed of highly vascular primitive-appearing mesenchymal cells with low nuclear grade and low mitotic activity embedded in a distinctive myxoid to myxochondroid matrix and exhibiting "grungy" or flocculent calcification. Other features include microcystic change, mature fat, chondroid or osteoid-like matrix, and woven bone [12, 13]. The pathological findings of this patient are consistent with this.

Surgery is the only established, definitive treatment of TIO [14, 15]. However, the localization and diagnosis is very difficult because of the small size, hidden location and slow development of tumors, and they may appear in any mesenchymal tissue all over the body, including bone and soft tissue [16]. FGF-23 secreted by tumors is an important pathogenesis of TIO, and serum FGF-23 levels are elevated in the majority of TIO patients. Therefore, systemic segmental venous sampling of FGF-23 facilitates the location of responsible tumors, but it has not been widely used in clinical practice as an invasive examination [17]. Furthermore, serum Klotho measurement maybe explain if the FGF23 cause is independent or dependent on Klotho. Noninvasive imaging examination plays an increasingly prominent role in the localization of TIO. X-ray manifestations of TIO are not significantly different from other osteomalacia, which are typically characterized by blurred trabeculae, multiple false fracture lines or fractures, "double concave" changes in the vertebral body and "triangular" changes in the pelvis [18]. CT and MRI can find hidden fracture and intraosseous edema, and make suggestive diagnosis for adult hypophosphorus osteomalacia patients who have ruled out other causes, but lack specificity [19, 20]. Besides, the specificity and sensitivity of fluorodeoxyglucose-positron emission tomography-computed tomography (^{18}F-FDG PET/CT) is also poor because PMT is mostly benign with low metabolic activity [21].

Since most responsible tumors are mesenchymal tissue derived and express the SSTR, SSTR-based functional PET/CT has been used successfully to detect TIO tumors. ^{111}In-pentetreotide or octreotide is the first approved radioactive drug for neuroendocrine tumor (NETs) imaging. Its high affinity for SSTR2 and SSTR5 makes ^{111}In-pentetreotide single-photon emission computed tomography (Octreoscan-SPECT/CT) useful for the localized diagnosis of TIO [22, 23]. 1,4,7,10-tetraazacyclododecane-1,4,7,10-tetraacetic acid tyrosine-3-octreotate (DOTATATE) is a radionuclide labeled somatostatin analogue, which is mainly used as PET or PET/CT imaging agent for the location diagnosis of SSTR positive NETs. ^{68}Ga-DOTATATE, like octreotide, is an antagonist of the SSTR, which upon receptor binding is internalized resulting in accumulation of radioactivity in tumor cells [24]. ^{68}Ga-DOTATATE PET/CT has been proved to be superior to Octreoscan-SPECT/CT for possible reasons: (1) ^{68}Ga-DOTATATE has higher affinity for SSTR2 and SSTR5 than octreotide [25, 26]; (2) PET/CT provides better spatial resolution than SPECT/CT [23, 27]. In addition, ^{68}Ga-DOTATATE imaging has advantages in terms of shorter acquisition time and lower radiation exposure because of its short half-life of 68 minutes, compared with 2.8 days for ^{111}In, the isotope used in Octreoscan-SPECT/CT imaging. ^{68}GA-DOTATATE PET/CT maximum standardized uptake value (SUV max)

also correlates with the clinical and pathologic features of NETs and is an accurate prognostic index [28]. In this case, ^{68}Ga-DOTATATE PET/CT demonstrated abnormal density of left middle and upper tibia with increased SSTR expression, thus successfully locating the tumor.

At present, TIO is mostly reported to start in middle age. However, the onset age of this case was prepubescent (12 years old), which is obviously younger than majority of reported cases. Thus it needs to be differentiated from hereditary hypophosphatemia, mainly including: (1) X-linked hypophosphacemic rickets (XLHR); (2) autosomal dominant hypophosphatemic rickets (ADHR); (3) autosomal-recessive hypophosphatemic rickets (ARHR) [29]. Although ADHR, ARHR, and XLHR are biochemically indistinguishable from TIO, they are the hereditary disease caused by gene mutation, often have a family history [30]. Whereas TIO is a paraneoplastic syndrome caused by tumors, and there are responsible tumors in vivo. A definitive diagnosis can be made by genetic testing when necessary. TIO also needs to be differentiated from primary hyperparathyroidism, primary osteoporosis, multiple myeloma, symptomatic Tarlov cysts, Fanconi's syndrome, and drug-induced hypophosphorous osteomalacia [2].

This patient was diagnosed with PCOS 3 years ago, while sex hormones returned to normal 5 days after surgery. It indicates the possible association between PCOS and TIO. However, as far as we know, its specific mechanism remains to be elucidated. Previous studies have found that $1,25(OH)_2D$ stimulates aromatase activity [31, 32], down-regulates estrogen receptor abundance and suppresses estrogen effect in human breast cancer cells [33], and up-regulates androgen receptor gene expression in prostate cancer cells [34]. Thus, vitamin D may play a role in the pathophysiologic mechanism of PCOS by influencing the balance between androgens with estrogens. Another possible pathway is apoptosis, $1,25(OH)_2D$ and calcium may be necessary for normal ovarian follicular formation. Loss of apoptotic mechanisms or overexpression of anti-apoptotic factors may lead to the appearance of polycystic ovary [35, 36]. In addition, in women with PCOS, serum levels of phosphorus were found to be negatively correlated with insulin resistance [37].

Neutral phosphorus solution and $1,25(OH)_2D$ replacement therapy can be given when TIO responsible tumors cannot be localized or completely resected. Serum phosphorus and symptoms can be improved to some extent, but cannot be cured [6]. The use of octreotide in TIO patients has been abandoned, as modulation of the somatostatin receptor using this somatostatin analogue has not been shown to affect the tumor mass or the phosphate metabolism [38, 39]. FGF-23 secreted by responsible tumors is the key hormone regulating renal phosphorus transport and bone mineralization. Inhibition of FGF-23 is an emerging treatment of unresectable TIO, such as FGF-23 antibodies, FGF-receptor inhibitors and mitogen-activated protein kinase (MAPK) inhibitors [40, 41]. However, whether or not these drugs, of which several are in development, will be safe and effective treatments for TIO remains to be seen, but they clearly hold promise.

TIO, as a rare paraneoplastic syndrome, is easy to be misdiagnosed. When patients develop unexplained progressive multiple bone pain, muscle weakness, hypophosphatemia and elevated alkaline phosphatase, the possibility of TIO should be considered. ^{68}Ga-DOTATATE PET/CT is recommended for the location of responsible tumors. Surgical removal and close follow-up are essential for the treatment of TIO. Patients unable to undergo surgery can be treated with neutral phosphorus solution and $1,25(OH)_2D$.

Abbreviations

TIO: Tumor-related osteomalacia; PMT: Phosphaturia stromal tumor; FGF23: Fibroblast growth factor 23; DXA: Dual-energy X-ray absorptiometry; PCOS: Polycystic ovary syndrome; PINP: Procollagen I N terminal peptide; CT: Computed tomography; MRI: Magnetic resonance imaging; ^{99m}Tc-MDP: ^{99m}Tc-methylene diphosphonate; DOTATATE: 1,4,7,10-tetraazacyclododecane-1,4,7,10-tetraacetic acid tyrosine-3-octreotate; SSTR: Somatostatin receptors; SPECT/CT: Single-photon emission computed tomography; ^{18}F FDG-PET/CT: Fluorodeoxyglucose-positron emission tomography-computed tomography; ALP: Alkaline phosphatase; NETs: Neuroendocrine tumor; SUV max: Maximum standardized uptake value; XLHR: X-linked hypophosphacemic rickets; ADHR: Autosomal dominant hypophosphatemic rickets; ARHR: Autosomal-recessive hypophosphatemic rickets; MAPK: Mitogen-activated protein kinase.

Acknowledgements

We felt deeply grateful for the patient for her generous sharing.

Authors' contributions

YX and QW conceived this study. LJ and LX collected clinical data. QQT, JHZ, PJY and YM analyzed data. LJ and QQT wrote the manuscript. YX, QW and CLG made manuscript revision. All authors contributed to the intellectual content of the manuscript. The author(s) read and approved the final manuscript.

Funding

This work was supported by the Natural Science Foundation of China [grant numbers 81900764, 81970676]; Sichuan Science and Technology Program [grant numbers 2020YFS0456, 2021JDJQ0043]; Luzhou-Southwest Medical University cooperation project [grant number 2020LZXNYDJ32]; and Suining First People's Hospital-Southwest Medical University cooperation project [grant number 2021SNXNYD01]. The funding bodies played no role in the design of the study and collection, analysis, and interpretation of data and in writing the manuscript.

Availability of data and materials

The datasets used and/or analysed during the current study are available from the corresponding author on reasonable request.

Declarations

Ethics approval and consent to participate

Not applicable.

Consent for publication
Written informed consent for publication of her clinical details and clinical images was obtained from the patient. A copy of the consent form is available for review by the Editor of this journal.

Competing interests
The authors declare that they have no competing interests.

Author details
[1]Department of Endocrinology and Metabolism, The Affiliated Hospital of Southwest Medical University, Luzhou 646000, Sichuan, China. [2]Cardiovascular and Metabolic Diseases Key Laboratory of Luzhou, The Affiliated Hospital of Southwest Medical University, Luzhou, Sichuan, P.R. China. [3]Sichuan Clinical Research Center for Nephropathy, The Affiliated Hospital of Southwest Medical University, Luzhou, Sichuan, P.R. China. [4]Metabolic Vascular Disease Key Laboratory of Sichuan Province, The Affiliated Hospital of Southwest Medical University, Luzhou, Sichuan, P.R. China.

Received: 20 November 2021 Accepted: 15 June 2022
Published online: 08 July 2022

References

1. Takashi Y, Kinoshita Y, Ito N, Taguchi M, Takahashi M, Egami N, et al. Tumor-induced Osteomalacia caused by a parotid tumor. Intern Med. 2017;56(5):535–9.
2. Minisola S, Peacock M, Fukumoto S, Cipriani C, Pepe J, Tella SH, et al. Tumour-induced osteomalacia. Nat Rev Dis Primers. 2017;3:17044.
3. McCance RA. Osteomalacia with Looser's nodes (Milkman's syndrome) due to a raised resistance to vitamin D acquired about the age of 15 years. Q J Med. 1947;16(1):33–46.
4. Florenzano P, Hartley IR, Jimenez M, Roszko K, Gafni RI, Collins MT. Tumor-induced Osteomalacia. Calcif Tissue Int. 2021;108(1):128–42.
5. Feng J, Jiang Y, Wang O, Li M, Xing X, Huo L, et al. The diagnostic dilemma of tumor induced osteomalacia: a retrospective analysis of 144 cases. Endocr J. 2017;64(7):675–83.
6. Hautmann AH, Hautmann MG, Kölbl O, Herr W, Fleck M. Tumor-induced Osteomalacia: an up-to-date review. Curr Rheumatol Rep. 2015;17(6):512.
7. Hautmann AH, Schroeder J, Wild P, Hautmann MG, Huber E, Hoffstetter P, et al. Tumor-induced Osteomalacia: increased level of FGF-23 in a patient with a Phosphaturic Mesenchymal tumor at the tibia expressing Periostin. Case Rep Endocrinol. 2014;2014:729387.
8. Kuro-O M. The Klotho proteins in health and disease. Nat Rev Nephrol. 2019;15(1):27–44.
9. Kinoshita Y, Takashi Y, Ito N, Ikegawa S, Mano H, Ushiku T, et al. Ectopic expression of Klotho in fibroblast growth factor 23 (FGF23)-producing tumors that cause tumor-induced rickets/osteomalacia (TIO). Bone Rep. 2019;10:100192.
10. Hu MC, Shi M, Zhang J, Addo T, Cho HJ, Barker SL, et al. Renal production, uptake, and handling of circulating αKlotho. J Am Soc Nephrol. 2016;27(1):79–90.
11. Folpe AL, Fanburg-Smith JC, Billings SD, Bisceglia M, Bertoni F, Cho JY, et al. Most osteomalacia-associated mesenchymal tumors are a single histopathologic entity: an analysis of 32 cases and a comprehensive review of the literature. Am J Surg Pathol. 2004;28(1).
12. Kumar R, Folpe AL, Mullan BP. Tumor-induced Osteomalacia. Transl. Endocrinol Metab. 2015;7:3.
13. Agaimy A, Michal M, Chiosea S, Petersson F, Hadravsky L, Kristiansen G, et al. Phosphaturic Mesenchymal tumors: Clinicopathologic, Immunohistochemical and molecular analysis of 22 cases expanding their morphologic and Immunophenotypic Spectrum. Am J Surg Pathol. 2017;41(10):1371–80.
14. Sun Z-j, Jin J, Qiu G-x, Gao P, Liu Y. Surgical treatment of tumor-induced osteomalacia: a retrospective review of 40 cases with extremity tumors. BMC Musculoskelet Disord. 2015;16:43.
15. Chong WH, Andreopoulou P, Chen CC, Reynolds J, Guthrie L, Kelly M, et al. Tumor localization and biochemical response to cure in tumor-induced osteomalacia. J Bone Miner Res. 2013;28(6):1386–98.
16. Kawai S, Ariyasu H, Furukawa Y, Yamamoto R, Uraki S, Takeshima K, et al. Effective localization in tumor-induced osteomalacia using Ga-DOTATOC-PET/CT, venous sampling and 3T-MRI. Endocrinol Diabetes Metab Case Rep. 2017;2017.
17. Andreopoulou P, Dumitrescu CE, Kelly MH, Brillante BA, Cutler Peck CM, Wodajo FM, et al. Selective venous catheterization for the localization of phosphaturic mesenchymal tumors. J Bone Miner Res. 2011;26(6):1295–302.
18. Kawthalkar AS, Janu AK, Deshpande MS, Gala KB, Gulia A, Puri A. Phosphaturic Mesenchymal tumors from head to toe: imaging findings and role of the radiologist in diagnosing tumor-induced Osteomalacia. Indian J Orthop. 2020;54(2):215–23.
19. Nakanishi K, Sakai M, Tanaka H, Tsuboi H, Hashimoto J, Hashimoto N, et al. Whole-body MR imaging in detecting phosphaturic mesenchymal tumor (PMT) in tumor-induced hypophosphatemic osteomalacia. Magn Reson Med Sci. 2013;12(1):47–52.
20. Yang M, Doshi KB, Roarke MC, Nguyen BD. Molecular imaging in diagnosis of tumor-induced Osteomalacia. Curr Probl Diagn Radiol. 2019;48(4):379–86.
21. Agrawal K, Bhadada S, Mittal BR, Shukla J, Sood A, Bhattacharya A, et al. Comparison of 18F-FDG and 68Ga DOTATATE PET/CT in localization of tumor causing oncogenic osteomalacia. Clin Nucl Med. 2015;40(1).
22. Wild D, Mäcke HR, Waser B, Reubi JC, Ginj M, Rasch H, et al. 68Ga-DOTANOC: a first compound for PET imaging with high affinity for somatostatin receptor subtypes 2 and 5. Eur J Nucl Med Mol Imaging. 2005;32(6):724.
23. Breer S, Brunkhorst T, Beil FT, Peldschus K, Heiland M, Klutmann S, et al. 68Ga DOTA-TATE PET/CT allows tumor localization in patients with tumor-induced osteomalacia but negative 111In-octreotide SPECT/CT. Bone. 2014;64:222–7.
24. Virgolini I, Ambrosini V, Bomanji JB, Baum RP, Fanti S, Gabriel M, et al. Procedure guidelines for PET/CT tumour imaging with 68Ga-DOTA-conjugated peptides: 68Ga-DOTA-TOC, 68Ga-DOTA-NOC, 68Ga-DOTA-TATE. Eur J Nucl Med Mol Imaging. 2010;37(10):2004–10.
25. Houang M, Clarkson A, Sioson L, Elston MS, Clifton-Bligh RJ, Dray M, et al. Phosphaturic mesenchymal tumors show positive staining for somatostatin receptor 2A (SSTR2A). Hum Pathol. 2013;44(12):2711–8.
26. Reubi JC, Schär JC, Waser B, Wenger S, Heppeler A, Schmitt JS, et al. Affinity profiles for human somatostatin receptor subtypes SST1-SST5 of somatostatin radiotracers selected for scintigraphic and radiotherapeutic use. Eur J Nucl Med. 2000;27(3):273–82.
27. Hofman MS, Lau WF, Hicks RJ. Somatostatin receptor imaging with 68Ga DOTATATE PET/CT: clinical utility, normal patterns, pearls, and pitfalls in interpretation. Radiographics : a review publication of the Radiological Society of North America. Inc. 2015;35(2):500–16.
28. Campana D, Ambrosini V, Pezzilli R, Fanti S, Labate AM, Santini D, et al. Standardized uptake values of (68)Ga-DOTANOC PET: a promising prognostic tool in neuroendocrine tumors. J Nuclear Med. 2010;51(3):353–9.
29. Jagtap VS, Sarathi V, Lila AR, Bandgar T, Menon P, Shah NS. Hypophosphatemic rickets. Indian J Endocrinol Metab. 2012;16(2):177–82.
30. Bacchetta J, Bardet C, Prié D. Physiology of FGF23 and overview of genetic diseases associated with renal phosphate wasting. Metabolism. 2020;103S:153865.
31. Lou Y-R, Murtola T, Tuohimaa P. Regulation of aromatase and 5alpha-reductase by 25-hydroxyvitamin D(3), 1alpha,25-dihydroxyvitamin D(3), dexamethasone and progesterone in prostate cancer cells. J Steroid Biochem Mol Biol. 2005;94(1–3):151–7.
32. Enjuanes A, Garcia-Giralt N, Supervia A, Nogués X, Mellibovsky L, Carbonell J, et al. Regulation of CYP19 gene expression in primary human osteoblasts: effects of vitamin D and other treatments. Eur J Endocrinol. 2003;148(5):519–26.
33. Swami S, Krishnan AV, Feldman D. 1alpha,25-Dihydroxyvitamin D3 downregulates estrogen receptor abundance and suppresses estrogen actions in MCF-7 human breast cancer cells. Clin Cancer Res. 2000;6(8):3371–9.
34. Zhao XY, Ly LH, Peehl DM, Feldman D. 1alpha,25-dihydroxyvitamin D3 actions in LNCaP human prostate cancer cells are androgen-dependent. Endocrinology. 1997;138(8):3290–8.
35. Homburg R, Amsterdam A. Polysystic ovary syndrome--loss of the apoptotic mechanism in the ovarian follicles? J Endocrinol Investig. 1998;21(9):552–7.
36. Das M, Djahanbakhch O, Hacihanefioglu B, Saridogan E, Ikram M, Ghali L, et al. Granulosa cell survival and proliferation are altered in polycystic ovary syndrome. J Clin Endocrinol Metab. 2008;93(3):881–7.

37. Mahmoudi T, Gourabi H, Ashrafi M, Yazdi RS, Ezabadi Z. Calciotropic hormones, insulin resistance, and the polycystic ovary syndrome. Fertil Steril. 2010;93(4):1208–14.
38. Nair A, Chakraborty S, Dharmshaktu P, Tandon N, Gupta Y, Khadgawat R, et al. Peptide receptor radionuclide and Octreotide: a novel approach for metastatic tumor-induced Osteomalacia. J Endocr Soc. 2017;1(6):726–30.
39. Ishii A, Imanishi Y, Kobayashi K, Hashimoto J, Ueda T, Miyauchi A, et al. The levels of somatostatin receptors in causative tumors of oncogenic osteomalacia are insufficient for their agonist to normalize serum phosphate levels. Calcif Tissue Int. 2010;86(6):455–62.
40. Beenken A, Mohammadi M. The FGF family: biology, pathophysiology and therapy. Nat Rev Drug Discov. 2009;8(3):235–53.
41. Ranch D, Zhang MY, Portale AA, Perwad F. Fibroblast growth factor 23 regulates renal 1,25-dihydroxyvitamin D and phosphate metabolism via the MAP kinase signaling pathway in Hyp mice. J Bone Miner Res. 2011;26(8):1883–90.

Publisher's Note

Springer Nature remains neutral with regard to jurisdictional claims in published maps and institutional affiliations.

Ready to submit your research? Choose BMC and benefit from:

- fast, convenient online submission
- thorough peer review by experienced researchers in your field
- rapid publication on acceptance
- support for research data, including large and complex data types
- gold Open Access which fosters wider collaboration and increased citations
- maximum visibility for your research: over 100M website views per year

At BMC, research is always in progress.

Learn more biomedcentral.com/submissions